MULTISTABILITY OF SYNCHRONOUS REGIMES IN OSCILLATORY ENSEMBLES

A.K.Kryukov, G.V.Osipov, A.V.Polovinkin and J.Kurths

***Abstract*— We study synchronous behavior in ensembles of locally coupled nonidentical Bonhoeffer - van der Pol oscillators. We show that in a chain of N elements 2^{N-1} different regimes of global synchronization are possible.**

I. INTRODUCTION

The understanding of principles of functioning of the human neuronal system and algorithms of information processing in neuron systems is an important actual challenge. Answers to these problems will have an immediate impact on the creation of highly efficient and low cost artificial neuron systems which are capable to solve tasks, apparent now as extremely complex [1], [2]. There are already first solutions in this direction demonstrating the potentials of artificial networks constructed by analogy with neuron systems. For example, it is processing of threads of multimedia data, including tasks of recognition of texts and images, optimum management of complex structures, brain-machine interactions etc.

One basic feature of ensembles of neurons in the central and peripheral nervous systems, or in cardiac tissue is there ability to synchronization [2-12]. Therefore, the study of synchronization in chains and networks of elements simulating self-oscillatory activity of neurons and cardiac cells is extremely important. In this paper we investigate synchronization in small (two and three elements) and large (chain) ensembles of coupled neuron-like oscillators. We demonstrate that such ensembles generate multistability of synchronous regimes. In dependence on the initial conditions in a chain of N coupled oscillators, 2^{N-1} synchronous regimes are possible. For $N = 2$ the existence of in-phase and anti-phase regimes is proved analytically. Numerical simulations show the appearance of four different synchronous regimes for $N = 3$. In large ensembles different regimes of global and cluster synchronization are found.

II. MODEL

In this paper we investigate a chain of locally diffusively coupled Bonhoeffer - van der Pol (BvdP) oscillators as a model of a neuron network [7]:

$$\begin{cases} \dot{x}_j = F_j(x_j, y_j) + d(x_{j+1} - 2x_j + x_{j-1}), \\ \dot{y}_j = G_j(x_j), \\ j = 1, ..., N, \end{cases} \quad (1)$$

where $F_j(x_j, y_j) = x_j - 1/3x_j^3 - y_j$, $G_j(x_j) = \varepsilon(x_j - a_j)$, N is the number of elements in the chain, and d is the coupling between the elements, $\varepsilon << 1$, $0 < a_j < 1$. We consider slightly nonidentical oscillators, which have small parameter mismatches $\Delta_{i,j} = a_i - a_j$. Free-end boundary conditions are taken. Because $\varepsilon << 1$ is very small, all oscillations in (1) can be divided in slow and fast motions. From a physiological point of view, the fast variable x can be considered as a voltage, but the slow variable y - as a gating or recovery variable. Therefore, the cooperative behavior of neuronal nets or cardiac tissue can be at least qualitatively reproduced by a model of coupled BvdP oscillators. In [12] this oscillator were successfully used as individual cell for modelling the frequency entrainment of heart pacemakers. Collective dynamics of synaptically coupled BvdP neurons was studied in [13].

III. SINGLE NEURON

For a single element:

$$\begin{cases} \dot{x} = x - y - \frac{x^3}{3}, \\ \dot{y} = \varepsilon(x + a), \end{cases} \quad (2)$$

there is one unstable steady state $(\bar{x}, \bar{y}) = (-a, \frac{a^3}{3} - a)$. It is (i) a focus if $a > \sqrt{1 - 2\sqrt{\varepsilon}}$, and (ii) a node if $a < \sqrt{1 - 2\sqrt{\varepsilon}}$). There exists also a stable limit cycle. Because of the smallness of ε it consists of fast and slow parts. A typical phase portrait is shown in a Fig.1a. Here $h_-(x)$ and $h_+(x)$ are the left resp. right steady parts and $h_0(x)$ is the unstable part of the curve of slow movements, correspondingly.

IV. TWO COUPLED NEURONS

For some fixed parameters there are two limit cycles in a pair of coupled elements. These cycles correspond to *in-phase* and *anti-phase* synchronous regimes. For the analytical proof of this fact for $a_1 \approx a_2$, we consider a piece-wise linear approximation of the functions $F_{1,2}$ (Fig.1b):

$$F_i = \begin{cases} \frac{-4}{3}x_i - 2 - y_i, & for \quad x_i \le -1, \\ \frac{2}{3}x_i - y_i, & for \quad -1 < x_i < 1, \\ \frac{-4}{3}x_i + 2 - y_i, & for \quad x_i \ge 1. \end{cases} \quad (3)$$

This work is done at financial support RFBR-NSC, project 05-02-90567 and RFBR-MF project 05-02-19815 and RFBR project 06-02-16596. G.O. and J.K. acknowledges support of EU-Network BioSim, Contract No. LSHB-CT-2004-005137

A.K.Kryukov, G.V.Osipov and A.V.Polovinkin are with Radiophysical department, University of Nizhny Novgorod, Gagarin ave. 23, 603950 Nizhny Novgorod, Russia; alkryukov@gmail.com, osipov@rf.unn.ru, polovinkin@rf.unn.ru

J.Kurths is with Institute of Physics, University Potsdam, 10, Am Neuen Palais, D-14415, Potsdam, Germany; juergen@agnld.uni-potsdam.de

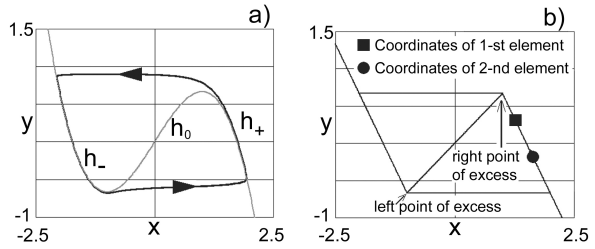

Fig. 1. a). Phase portrait of system (2). b). In-phase regime at piece-wise linear approximation of the functions $F_{1,2}$ given according to (3).

These functions have two extrema: the right extreme $y_{1,2} = 2/3 + d(x_{2,1} - x_{1,2})$, and the left extreme $y_{1,2} = -2/3 + d(x_{2,1} - x_{1,2})$. Under the general assumption that the switching time from $h_{\pm}(x)$ to $h_{\mp}(x)$ is extremely small, in the steady regime there are four possible types of mutual arrangements of both elements:

i). both are situated in $h_+(x)$;

ii). both are situated in $h_-(x)$;

iii). the representing point of the first element is situated in $h_+(x)$, and the representing point of the second element - in $h_-(x)$;

iv). the representing point of the first element is situated in $h_-(x)$, and the representing point of the second element - in $h_+(x)$.

In our study, if most part of the period of the limit cycle: (a) variant i) or ii) is realized, then an in-phase synchronous regime takes place, and (b) variant iii) or iv) is realized, then an anti-phase synchronous regime sets in. Note that for $a_1 = a_2$ for an in-phase regime $_1 = _2$, $y_1 = y_2$, and for an anti-phase regime the lag between two time series is equal to $T/2$, where T is the period of the oscillations.

Let us study the first variant: both elements are on $h_+(x)$ (see Fig.1b). After substitution $\tau = \varepsilon t$ at vanishing ε, according to (3) we get the simplified model:

$$\begin{cases} 0 &= F_1(x_1, x_2, y_1, y_2, d), \\ \dfrac{dy_1}{d\tau} &= x_1 + a_1, \\ 0 &= F_2(x_1, x_2, y_1, y_2, d), \\ \dfrac{dy_2}{d\tau} &= x_2 + a_2. \end{cases} \tag{4}$$

Solving this linear system, we find both limit cycles. To do this, we build the mapping $df_{n+1}(df_n)$, where n corresponds to the n-th passing of the limit cycle, and $df_n = y_1^n - y_2^n$. Without loosing generality, let us consider the following case. Let y_1^n, y_2^n be the values of y_1 and y_2 on the n-th passing of the limit cycle. Then the first element just comes to the line $h_-(x)$. The state y_2^n of the second element can be arbitrary on the lines $h_-(x)$ or $h_+(x)$. The state y_1^n of the first element is defined through y_2^n. Let us assume that the second element is located on the $h_+(x)$. Then

$$y_1^n = 2/3 + d(x_2 - x_1) = \hat{d}^{-1}(4\bar{d}/3 - dy_2^n), \tag{5}$$

where $\bar{d} = 2/3 + d$ and $\hat{d} = 4/3 + d$.

Let in the moment $\tau = t_1$ the second element jumps to the line $h_-(x)$. Then, solving system (4), one obtains for $y_1(t_1)$ and $y_2(t_1)$:

$$y_1^{-+}(t_1) = \left[\tfrac{1}{2}(y_1^n - y_2^n) + 2 - (a_1 - a_2)\bar{d}\right]\exp(-\tfrac{t_1}{2\bar{d}}) + \left[\tfrac{1}{2}(y_1^n + y_2^n) - \tfrac{2}{3}(a_1 + a_2)\right]\exp(-\tfrac{3t_1}{4}) - 2 - da_2 + \hat{d}a_1, \tag{6}$$

$$y_2^{-+}(t_1) = \left[\tfrac{1}{2}(y_2^n - y_1^n) - 2 + (a_1 - a_2)\bar{d}\right]\exp(-\tfrac{t_1}{2\bar{d}}) + \left[\tfrac{1}{2}(y_1^n - y_2^n) - \tfrac{2}{3}(a_1 + a_2)\right]\exp(-\tfrac{3t_1}{4}) + 2 - da_2 + \hat{d}a_1. \tag{7}$$

In expressions (6) and (7) the index "$-+$" means, that the first element is on the line $h_-(x)$, and the second one on the line $h_+(x)$. From another side, because the fact that at $\tau = t_1$ the second element jumps to the line $h_-(x)$ we have:

$$y_2(t_1) = \frac{2}{3} + \frac{d}{2\bar{d}}(y_2(t_1) - y_1(t_1) - 4) \tag{8}$$

Comparing (7) and (8) and taking into account (6), we can find the moment t_1. Now both elements are on the line $h_-(x)$. The corresponding values $y_1(\tau)$ and $y_2(\tau)$ can be calculated:

$$y_1^{--}(\tau) = \left[\tfrac{1}{2}(y_1(\tau_0) - y_2(\tau_0)) - (a_1 - a_2)\bar{d}\right]\exp(-\tfrac{\tau-\tau_0}{2\bar{d}}) + \left[\tfrac{1}{2}(y_1(\tau_0) + y_2(\tau_0)) + 2 - \tfrac{2}{3}(a_1 + a_2)\right]\exp(-\tfrac{3}{4}(\tau - \tau_0)) - 2 - da_2 + \hat{d}a_1, \tag{9}$$

$$y_1^{--}(\tau) = \left[\tfrac{1}{2}(y_2(\tau_0) - y_1(\tau_0) + (a_1 - a_2)\bar{d}\right]\exp(-\tfrac{\tau-\tau_0}{2\bar{d}}) + \left[\tfrac{1}{2}(y_1(\tau_0) + y_2(\tau_0)) + 2 - \tfrac{2}{3}(a_1 + a_2)\right]\exp(-\tfrac{3}{4}(\tau - \tau_0)) - 2 - da_1 + \hat{d}a_2, \tag{10}$$

Each element can reach the left extreme before the other element. This depends on the initial conditions and the parameters. Let at $\tau = t_2$ one of the elements reaches the left extreme. Then $y_1(t_2), y_2(t_2)$ can be obtained from (9) and (10). From another side, we can use the fact that one element at $\tau = t_2$ is located in the left extreme. Therefore, we can define the moment t_2. If we move further along the cycle, then we can obtain (i) the moment where the first element jumps again from the line $h_+(x)$ to the line $h_-(x)$, and (ii) the values y_1^{n+1} and y_2^{n+1}. Therefore, we can build the mapping $df_{n+1}(df_n)$. This mapping at $d = 0.002$, $a_1 = 0.995$, $a_2 = 0,994$ and at the initial state of the second element the $h_-(x)$ is presented in Fig.2a. It is visible, that there are two steady fixed points, each related to the certain synchronous regime. The fixed point in a vicinity of zero corresponds to an in-phase regime ($x_1 \approx x_2$); the point near $df(n) = 1.323$ corresponds to an anti-phase regime. Both

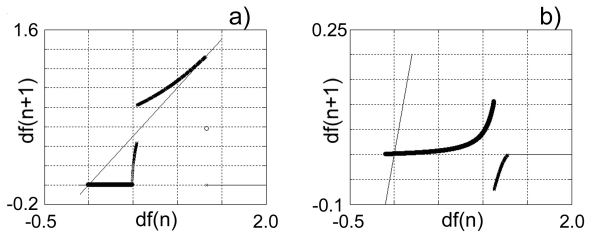

Fig. 2. Map $df_{n+1}(df_n)$. Initially the second element is located on $h_-(x)$. Parameters are: $a_1 = 0.995$, $a_2 = 0.994$, $\varepsilon = 0.02$ and: a) $d = 0.002$, b) $d = 0.05$.

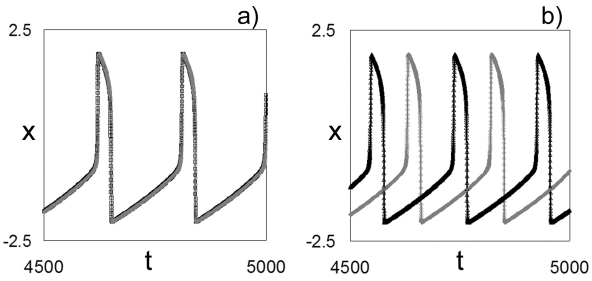

Fig. 3. Time series for in-phase (a), and anti-phase (b) regimes of system (1) for $N = 2$.

of these regimes appear if the coupling strength d becomes larger than some critical value. With further increase of d, the fixed point corresponding to an anti-phase regime disappears but the fixed point corresponding to an in-phase regime remains (Fig.2b). This means that for relatively large coupling only an in-phase synchronous regime exists.

These analytical results obtained for a linear approximation of the functions $F_{1,2}$ are tested in numerical experiment with model (1) for $N = 2$, $\varepsilon = 0.02$. This way we get the existence of in-phase and anti-phase synchronous regimes. The appropriate time series are given in Fig. 3a and 3b. It is necessary to note, that the anti-phase regime is realized not only in some intervals of the coupling parameter d, but in some interval of the difference of the parameters $a_2 - a_1$ too. In the case of a large difference $a_2 - a_1$, when even for one of the elements the time of movement along $h_+(x)$ is close to the time of movement along $h_-(x)$, the anti-phase regime disappears. Therefore, it is possible to assume that the strong difference between the times of two parts of slow movement is a reason for the existence of two (and very big for large ensembles) synchronous regimes. We have obtained the evolution of the observed frequencies $\omega_j = 2\pi/T_j$ vs. the parameter d. Here $T_j = 1/M \sum_{i=1}^{M} T_{ij}$,where $M \to \infty$, $j = 1, 2$, and T_{ij} is the sequence of time intervals between consecutive maxima of realization $x_j(t)$. In other words ω_j is an averaged frequency of the occurrence of maxima in the time series $x_j(t)$.

As our numerical experiments show, the in-phase and anti-phase regimes have strongly different observed frequencies. The frequency of the in-phase regime is close to the maximal of the individual frequencies of the uncoupled elements, but the frequency of the anti-phase regime goes to zero if d

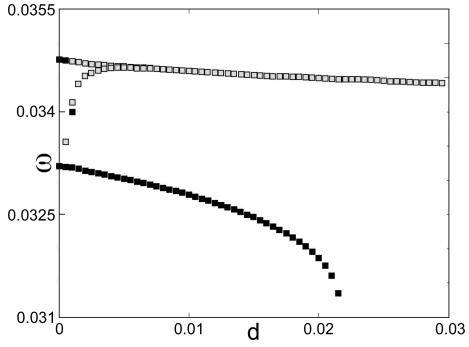

Fig. 4. Synchronization regimes in an ensemble of two coupled elements. Distribution of mean frequencies vs. coupling. Parameters are: $\varepsilon = 0.02$, $a_1 = 0.995$, $a_2 = 0.994$.

increases, and therefore, the anti-phase regime disappears (Fig. 4). It can be noticed, that for identical elements decreasing of this frequency can be estimated analytically. Thus, at $d > d_{cr}$ only the in-phase regime exists.

V. Three coupled elements

In an ensemble of three coupled elements the interval of coupling, in which four synchronous regimes can be realized in dependence on the initial conditions, is found: (i) in-phase regime ($x_1 \approx x_2 \approx x_3, y_1 \approx y_2 \approx y_3$) and three mixed regimes where two of the oscillators are synchronized in-phase

(ii) regime, for which $x_1 \approx x_2, y_1 \approx y_2$;

(iii) regime, for which $x_2 \approx x_3, y_2 \approx y_3$;

(iv) regime, for which $x_1 \approx x_3, y_1 \approx y_3$, in some sense this regime can be called anti-phase regime.

Therefore $2^{N-1} = 2^2 = 4$ synchronous regimes are possible. The lags between the time series $x_1(t), x_2(t), x_3(t)$ are non constant and can be changed in dependence on the parameters. Under some conditions the regime of splay-state occurs, for which the time between the maxima of the time series is close to $T/3$, where T is the period of the synchronous oscillations.

Dependence of the observed frequencies on coupling of three coupled elements is shown in Fig. 5. Each curve in the figure describes this dependence at one of the four regimes of global synchronization. In numerical experiment we've varied only initial conditions to obtain the synchronous regime which we need.

The mixed regimes are established at some frequency ω^s_{mix}, such that $\omega^s_{sp} < \omega^s_{mix} < \omega^s_{in}$, where $\omega^s_{sp}, \omega^s_{in}$ are the synchronization frequencies of the splay-state and the in-phase synchronous regimes, correspondingly. Mixed regimes exist in a wider interval of d than the splay state. With increasing d the mixed regimes disappear, and only the in-phase regime remains.

VI. Global and cluster synchronization in large ensembles

In order to study synchronization phenomena in large ensembles of neuron-like elements, we investigate a chain of 50 coupled oscillators with linearly distributed parameters a_j

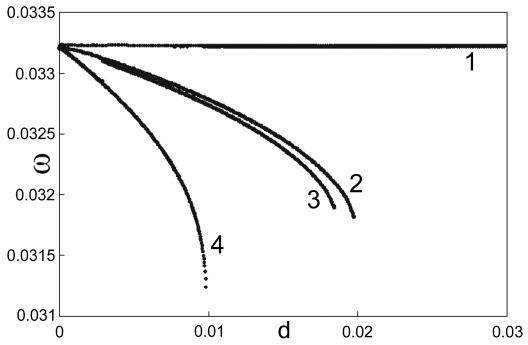

Fig. 5. Synchronization regimes in an ensemble of three coupled elements. Distribution of mean frequencies $\Omega_{1,2,3}$ vs. coupling. Curve 1 correspond to an in-phase synchronous regime (i). Curve 4 - to an anti-phase synchronous regime (iv). Curve 2 - to an mixed regime (ii). Curve 3 - to a mixed regime (iii). Parameters are: $\varepsilon = 0.02$, $a_1 = 0.995, a_2 = 0.99493, a_3 = 0.99486$.

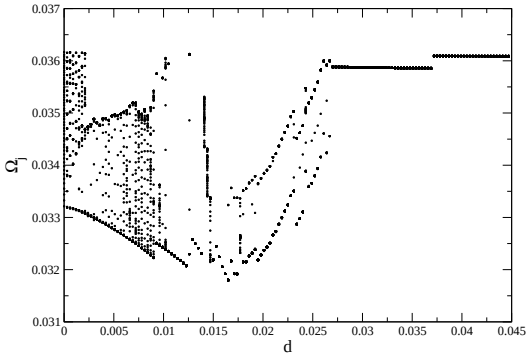

Fig. 6. Synchronization frequencies in the chain of 50 coupled elements for $a_1 = 0.995$, $\Delta a = 0.001$, $\varepsilon = 0.02$.

($a_j = a_1 + \Delta a(j-1)$). The results obtained in the previous sections allows us to suppose that in this chain for some parameters 2^{N-1} different regimes of global synchronization are possible. In numerical experiments several of such regimes were found (Fig. 6). The evolution of the synchronization frequencies for an increasing coupling parameter is similar to the evolution in the systems of two and three coupled elements. As in the previous numerical experiments, in the in-phase regime the synchronization frequency is close to the maximal of the individual frequencies. This regime remains with increasing d.

With an increase of coupling from 0 the formation of groups of synchronized neighboring elements, i.e. clusters of synchronization, appears. The number of clusters decreases with increasing d, and for $d \geq> 0.03$ global synchronization sets in (Fig. 7). The formation of synchronous clusters is observed for randomly distributed parameters a_j as well. [14].

VII. Conclusions

Basing on the received results it is possible to assume, that in a system of N locally diffusively coupled Bonhoeffer - Van der Pol oscillators for fixed values of parameters the number of different globally synchronous regimes can be equal to 2^{N-1}. This was numerically confirmed for N=3. An

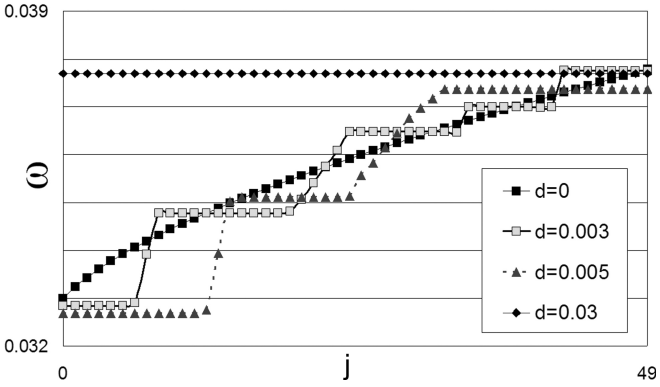

Fig. 7. Global ($d = 0.03$) and cluster synchronization in the chain of 50 coupled elements for $a_1 = 0.995$, $\Delta a = 0.001$, $\varepsilon = 0.02$.

analytical proof for the existence of two synchronous regimes was performed for N=2. In large ensembles a transition to global synchronization is accomplished with the formation of synchronization clusters. For relatively strong coupling, only the in-phase synchronous regime exists, which is realized on a frequency close to the maximal of the individual frequencies.

Many theoretical and experimental results show that synchronization phenomena play a very important role in brain activity. It is assumed that synchronous firing of neurons are an essentional mechanism for information processing. Therefore, the observed multistability of synchronous regimes may be useful by understanding of mechanisms of different brain functions including image storage and recognition, visual perception, memory processing, control of movement and posture.

References

[1] P. A. Tass *Phase resetting in Medicine and Biology* Springer, Berlin, 1999.

[2] E. Mosekilde, Yu. Maistrenko, and D. Postnov, *Chaotic Synchronization. Applications to Living Systems*, World Scientific, Singapore, 2002.

[3] Pikovsky A.S., Rosenblum M.G., and Kurths J. , Synchronization - A universal concept in Nonlinear Sciences, Cambridge University Press, Cambridge, 2001.

[4] Varona P., Torres J.J., Huerta R., Abarbanel H.D.I., and Rabinovich M.I., *Neural Networks*, vol.14, p.865, 2001.

[5] R. Eckhorn, R. Bauer, W. Jordan, M. Brosch, W. Kruse, M. Munk, and H.J. Reitboeck, Biol. Cybern., **60** 121 (1988).

[6] A.K. Engel, P. Knig, A.K. Kreiter, and W. Singer, Science, **252** 1177 (1991).

[7] Bonhoeffer K.F., *Naturwissenschaften*, vol.40, p.301, 1953.

[8] V.N. Murthy and E.E. Fetz, Proc. Natl. Acad. Sci. USA, **89** 5670 (1992).

[9] E.E. Verheijck, R. Wilders, R.W. Joyner, D.A.Golod, R. Kumar, H.J. Jongsma, L.N. Bouman, and A.C.G. van Ginneken, J. Gen. Physiol., **111** 95 (1998).

[10] D.C. Michaels, E.P. Matyas, and J. Jalife, Circ. Res., **61** 704 (1987).

[11] L. Glass, Nature, **410** 277 (2001).

[12] V. Torre, J.Theor.Biol., **61** 55 (1976).

[13] K. Tsumoto, T. Yoshinaga, and H. Kawakami, Phys. Rev. E **65** 036230 (2002).

[14] G. V. Osipov and M. M. Sushchik, Phys.Rev.E, **58**,7198, (1998).

[15] G. V. Osipov, A. S. Pikovsky, M. G. Rosenblum and J. Kurths, Phys.Rev. E **55**, 2353 (1997).